Progress of Theoretical Physics, Vol. 101, No. 4, April 1999

Distribution Phenomena in Continued Fractions and Logistic Map

Shuji OBATA and Shigeru OHKURO*

Physics Laboratory, Faculty of Science and Engineering
Tokyo Denki University, Hiki-gun, Saitama 350-0394, Japan
**Laboratory of Information and System Engineering*
Hachinohe Institute of Technology, Hachinohe 031-8501, Japan

(Received December 26, 1997)

We have been studying chaotic behavior and chaos-like behavior in continued fractions. In this paper, such chaos-like behavior is investigated in detail. This behavior originates in the complex numbers that determine the Cauchy distributions, where cyclic terms discretely appear at isolated parameter values. The distributions are formed along with alternate tangent functions that are dominated by the cyclic terms characterized by double-Markov processes. Finally, the probability densities of the logistic map are analyzed based on the Cauchy distributions, like state density calculations in solids.

§1. Introduction

In a separate paper,[1)] many types of chaotic and chaos-like behavior are observed in continued fractions, which are represented by the corresponding fractal structures like Bethe-Lattices (BL). In an electronic density calculation method employing a linear combination of atomic orbitals (LCAO), the Green's function can be formulated by a reverse matrix of a secular equation. The ij elements of the Green's function can be expressed in the form

$$G_{ij}(E) = \frac{1}{E - \Sigma_{ij}(x(E))}, \tag{1}$$

where Σ is the self-energy and E is an energy parameter. Within a BL approximation, the terms x are equated as self-consistent continued fractions.[1)] These corresponding structures become fractal trees[2)] (Cayley trees), where the interactions between ij elements, v_{ij}, become symmetric values: $v_{ij} = v_{ji}$.

In contrast to electronic interaction systems, interactions in other systems can be represented by asymmetric matrix elements ($v_{ij} \neq v_{ji}$). In such systems, the iterated values of the self-energies exhibit chaotic behavior as a characteristic of fractal structure systems.[2),3)] For example, a self-consistent continued fraction

$$x_{n+1} = \cfrac{R}{a - \cfrac{b}{c - x_n} - \cfrac{d}{e - x_n}} \tag{2}$$

becomes the expanded logistic map (LM). By fixing the parameters as $a = 0,\ b = 1,\ c = 0,\ d = -1$ and $e = 1$, one can obtain the LM equation.[3)-5)] On the contrary, the parameters become $b > 0,\ d > 0$ in the electronic systems.

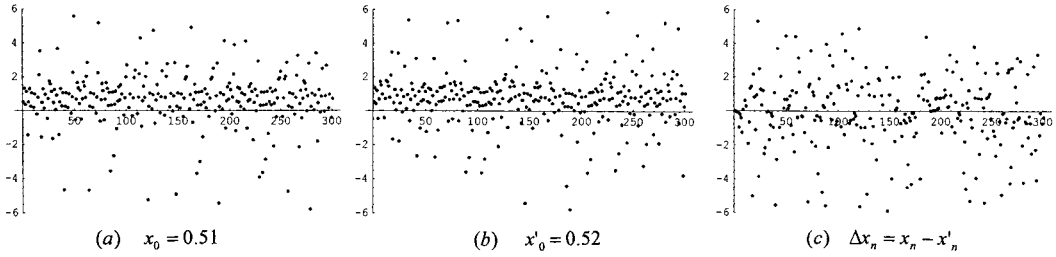

Fig. 1. Chaos-like sequences in the parallel continued fraction equation in Eq. (4). Small differences in starting values result in quite different sequences, as illustrated by (a) and (b), where $a = 0.281$, $b = 1.01$, $c = 1.5$ and $d = 2.5$ in Eq. (4). (c) The difference between the two sequences.

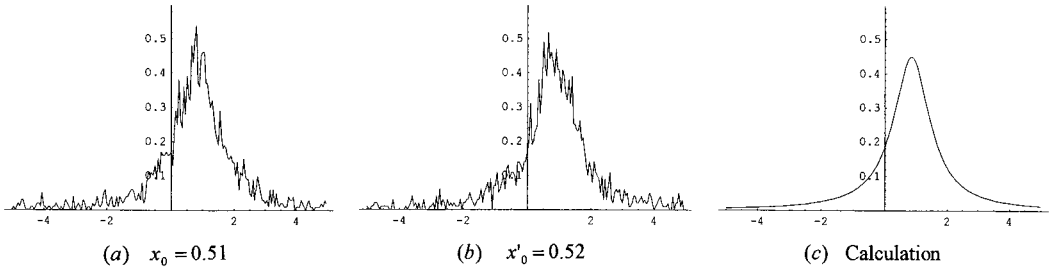

Fig. 2. The densities of the Cauchy distributions in the continued fractions. Figures (a) and (b) are the densities of $n = 2000$ iterations in Fig. 1(a) and (b), respectively. (c) The calculated distribution using the solution for the case $\xi = 0.852464$ and $\eta = 0.70837$.

To investigate chaos-like behavior in continued fractions for symmetric interaction systems, the simple continued fraction

$$x_{n+1} = \frac{a}{b - x_n} \tag{3}$$

is analyzed in detail in §2. The iterated terms in this equation satisfy several beautiful mathematical relations. The parallel continued fractions

$$x_{n+1} = \frac{a}{b - x_n} + \frac{c}{d - x_n} \quad \text{for} \quad a, c > 0 \tag{4}$$

exhibit chaos-like sequences, where small changes in starting values yield completely different distribution sequences, as seen in Fig. 1. These two sequences in Fig. 1 are distributed according to the same Cauchy distribution (as shown in Fig. 2), which is characterized by the complex number solution of the equation

$$x_{n+1} = x_n = \xi + i\eta. \tag{5}$$

This relation is satisfied in both equations (3) and (4).

In §2, a simple continued fraction is analyzed in terms of convergence, cycles and distributions. It is shown that, in the cyclic terms, double Markov process-numbers play an important role. The Cauchy distributions produced along with the tangent curves are dominated by these cyclic terms. This type of distribution sometimes appears in other chaos-like behavior.[6)]

In §3, the logistic map is studied using the same method of analysis used for the continued fractions. The chaotic areas are calculated using the attractor solutions of the Cauchy distributions, where repellor solutions are destroyed. The density of the map is calculated approximately in a theoretical approach based on the state density calculations in solids.

§2. A simple continued fraction

In this work, Eq. (3) is analyzed because of its simplicity. In these results, we can discover some beautiful relations inherent in continued fractions.

2.1. *The basic equation*

At the k-th iteration from the n-th step, the simple continued fraction can be transformed into

$$\begin{aligned} x_{n+k} &= \cfrac{a}{b-\cfrac{a}{b-\ddots\,\cfrac{a}{b-x_n}}} \\ &= \frac{A_k - C_k x_n}{B_k - D_k x_n}. \end{aligned} \tag{6}$$

At the i-th intermediate step of this transformation, the relation

$$\frac{A_i - C_i x_n}{B_i - D_i x_n} = \cfrac{a}{b-\cfrac{A_{i-1} - C_{i-1} x_n}{B_{i-1} - D_{i-1} x_n}} \tag{7}$$

is obtained. In this equation, the terms are inductively related as

$$\begin{aligned} A_i &= aB_{i-1}, \\ B_i &= bB_{i-1} - A_{i-1}, \\ C_i &= aD_{i-1}, \\ D_i &= bD_{i-1} - C_{i-1}. \end{aligned} \tag{8}$$

From these relations and the initial conditions

$$A_1 = a, \quad B_1 = b, \quad C_1 = 0, \quad D_1 = 1, \tag{9}$$

the expanded terms

$$\begin{aligned} C_i &= A_{i-1} = aB_{i-2}, \\ D_i &= B_{i-1} \end{aligned} \tag{10}$$

can all be rewritten in the double Markov sequence of B_i terms:

$$\begin{aligned} B_i &= bB_{i-1} - aB_{i-2}, \\ B_{-1} &= 0, \quad B_0 = 1. \end{aligned} \tag{11}$$

The continued terms are expanded as

$$\begin{aligned} B_1 &= b, \\ B_2 &= b^2 - a, \\ B_3 &= b(b^2 - 2a), \\ B_4 &= b^4 - 3ab^2 + a^2, \\ &\cdots. \end{aligned} \tag{11}'$$

This is an important result of the fundamental double Markov sequence. If we use the values $a = -1$ and $b = 1$ in B_k, then the famous Fibonacci sequence appears directly. In this way Eq. (6) can be rewritten as

$$x_{n+k} = q_k(x_n) = \frac{a(B_{k-1} - B_{k-2}x_n)}{B_k - B_{k-1}x_n}. \tag{12}$$

Now, with the relations

$$\begin{aligned} x_{n+k} &= x_n + \Delta_k, \\ x_n &= x. \end{aligned} \tag{13}$$

Equations (12) and (13) can be transformed into the basic quadratic equation for simple continued fractions:

$$\Delta_k = \frac{B_{k-1}(x^2 - bx + a)}{B_k - B_{k-1}x}. \tag{14}$$

Continued fractions can be analyzed using this equation.

The function $q(x)$ in Eq. (12) is expanded as follows by considering the change δ induced from a small shift ε:

$$x_{n+k} + \delta = q_k(x_n + \varepsilon) = q_k(x_n) + q_k'(x_n)\varepsilon + \cdots.$$

Using Eq. (10) and the value λ_k, this derivative is represented as

$$\begin{aligned} \lambda_k &= \frac{B_{k-1}}{B_k}, \\ q_k'(x) &= \frac{a\lambda_k^2 - b\lambda_k + 1}{(1 - \lambda_k x)^2}. \end{aligned} \tag{15}$$

This equation is needed for checking the attractor terms.

2.2. *Convergence (The case of $\Delta_k = 0$ for arbitrary k)*

Under the condition $B_{k-1} \neq 0$ in Eq. (14), convergent sequences with respect to x_1 appear in the continued fractions, where the quadratic equation satisfies the conditions

$$\begin{aligned} x^2 - bx + a &= 0, \\ 4a &\leq b^2. \end{aligned} \tag{16}$$

The solutions become real numbers:

$$x = \frac{b \pm \sqrt{b^2 - 4a}}{2} = \xi \pm \zeta$$
$$= x_1, x_2(|x_1| < |x_2|). \tag{17}$$

Between these two real solutions, the stable convergent value becomes x_1, which is near 0. Under the condition $\delta < \varepsilon$, substituting the value

$$\lambda_1 = \frac{B_0}{B_1} = \frac{1}{b} \tag{18}$$

into Eq. (12), we obtain the relation for the value of x_1

$$a = -x_1(b - x_1),$$
$$\left|\frac{\delta}{\varepsilon}\right| = |q_1'(x)| = \left|\frac{a}{(b - x_1)^2}\right| = \left|\frac{x_1}{b - x_1}\right|$$
$$= \left|\frac{(\xi \pm \zeta)}{\xi \mp \zeta}\right| = \left|\frac{x_1}{x_2}\right| < 1. \tag{19}$$

2.3. *Cycles (The case of $\Delta_k = 0$ for some k)*

In this section, the sequence λ_k in Eq. (14) is denoted by Λ_k as cyclic terms. We can obtain equations for cyclic sequences with k-time periods in the case $\Delta_k = 0$. Under the condition

$$x^2 - bx + a = (x - \xi)^2 + \eta^2 \neq 0, \tag{20}$$

the cycle equations are obtained from Eq. (14):

$$x_{n+k} = x_n,$$
$$\Lambda_k(a, b)(x^2 - bx + a) = 0, \tag{21}$$

where

$$\Lambda_k = B_{k-1}/B_k = 0. \tag{22}$$

The special equations $\Lambda_k = B_{k-1} = 0$ ($\lambda_k = 0$) can be expanded in a and b through iterations of Eq. (11):

$$\Lambda_3 = (b^2 - a)/b(b^2 - 2a),$$
$$\Lambda_4 = b(b^2 - 2a)/(b^4 - 3ab^2 + a^2),$$
$$\Lambda_5 = (b^4 - 3ab^2 + a^2)/B_5,$$
$$\cdots. \tag{23}$$

Several values of a determining these cycle conditions are listed in Fig. 3 using $r = 1/a$ for $b = 1$. The values of a are restricted in the range defined by

$$0 < r = \frac{1}{a} < 4 \tag{24}$$

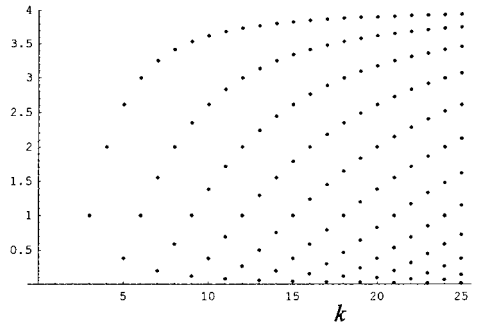

Fig. 3. Values $(1/a)$ of the cycle conditions for $b = 1$.

under the conditions of Eqs. (20)–(22). The value r has a similar role to that of R in the logistic map.

Here, it is shown that the cyclic terms are stable in the continued fractions. The fact that the quantity δ is equal to ε follows directly from $\lambda_k = 0$ in Eq. (15):

$$\left|\frac{\delta}{\varepsilon}\right| = |q_k'(x)| = 1. \tag{25}$$

This implies that the cycles are eternal at an arbitrary starting number x. For example, for the values

$$k = 3 \quad \text{and} \quad a = b = 1,$$

the arbitrary value of x follows a three-term cycle:

$$x, \quad \frac{1}{1-x}, \quad 1 - \frac{1}{x}, \quad x.$$

The values of λ_k nearly equal to 0 are very important in our study. This point is discussed in §2.4.

2.4. *Distribution (The case of $\Delta_k \neq 0$ for arbitrary k)*

2.4.1. Basic analysis

Under the conditions in Eq. (15)

$$\begin{aligned} &0 \neq |B_{k-1}| \ll 1, \\ &4a > b^2, \end{aligned} \tag{26}$$

$$\left|\lambda_k = \frac{B_{k-1}}{B_k}\right| \ll 1, \tag{27}$$

the value Δ_k of Eq. (14) becomes small but not 0. In this case, the attractor terms can be evaluated except for in the particular case

$$|1 - \lambda_k x| \ll 1 \rightarrow |q_k'(x)| \gg 1.$$

From Eqs. (20) and (26), the complex number solutions are obtained:

$$x = \xi \pm i\eta. \tag{5)(20}$$

This result allows us to conclude that the quadratic formula never becomes 0 for any real number x. This conclusion is very important in later arguments. "Nearly 0" is not "exactly 0", and the value x_{n+k} is never equal to x_n at any step k. This means that the x_n are ergodically distributed on the real axis under the condition of a small shift $\Delta_k \neq 0$. From the results of Fig. 3, it can be known that the cycle points linearly increase for every odd iteration step. These values of $1/a$ are distributed from 0 to 4 with roughly equal distances. This fact insures the existence of the condition in Eq. (26) for any values of a and b in large iteration steps.

At the k-th iteration from n, if the value x_{n+k} is close to x_n,

$$\begin{aligned} &x_{n+k} = x_n + \Delta_k, \\ &0 < |\Delta_k| \ll 1 \end{aligned} \tag{28}$$

B_k {0, 1, 1.01, 0.73815, 0.460762, 0.257248, 0.129909, 0.0586768, 0.0226358, 0.00631821, -7.67121×10^{-7}, -0.00178219, -0.0017998, -0.00131531, -0.000821007, -0.000458367, -0.000231467, -0.000104545, -0.0000403287, -0.0000112554, 2.73372×10^{-9}}

λ_k {0, 0.990099, 1.36829, 1.60202, 1.79112, 1.98022, 2.21397, 2.59222, 3.58263, -8236.26, 0.000430436, 0.990218, 1.36835, 1.60207, 1.79116, 1.98027, 2.21404, 2.59233, 3.58306, -4117.24, 0.000860685}

Fig. 4. B_k, and λ_k in the double Markov sequence. At $k = 10$, the value $\lambda_{10} = 0.00043$ appears for $a = 0.28195$ and $b = 1.01$.

and the value $|x\lambda_k|$ is not too large, Eq. (14) can be approximately rewritten as

$$\begin{aligned} &|B_{k-1}x| \ll |B_k|, \\ &\Delta_k \approx \lambda_k(x^2 - bx + a). \end{aligned} \tag{29}$$

Large x values appear with small probability in the continued fractions, and the effect of this appearance is suppressed by sufficiently small λ_k ($k \gg 1$) in Eq. (14). Figure 3, the distribution map of $1/a$ satisfying the equation $\lambda_k = 0$, indicates that the condition $\lambda_k \approx 0$ exists for large k and any value of a. An example of such cases can be illustrated by sequences of B_k and λ_k, as in Fig. 4. A small value of λ_k ($0.00043\cdots$) appears in the second sequence at the 10th iteration for $a = 0.281950$ and $b = 1.01$. If the value a is $0.281949\cdots$ and $\lambda_{10} = 0$, these continued fraction terms become cyclic. The value corresponding to this situation in Fig. 3 is $r = 3.618$ ($a = 0.2764$, $b = 1.0$) at $k = 10$. Thus, in the case that λ_k is nearly 0, the continued fractions are distributed as in Fig. 5, and they produce many tangent functions, which are discussed below.

The next step value in Eq. (28) is important for analyzing the "nearly 0" behavior:

$$x_{n+k+1} - x_{n+1} = \frac{a}{b - x_{n+k}} - \frac{a}{b - x_n} = \frac{a\Delta_k}{(b - x_{n+k})(b - x_n)}. \tag{28}'$$

In Eq. (28)′, the Δ_k value can become sufficiently small. From this result it is known that if a pair of almost equal values x_{n+k} and x_n exists, k-period sequences of the partial continued fractions behave similarly and appear alternately in the continued iterations as shown in Fig. 5.

For the k period plotting of x_{n+k} with small difference Δ_k, many smooth curves can be traced as in Fig. 5. A plus sign on Δ_k indicates an increasing step in the x_{k+n} tracing, while a minus sign indicates a decreasing step. Iteration lengths l_{full} of the tangent curves are calculated below, in Eqs. (36)–(38). In Fig. 5, the tangent functions of (a) can be traced by $k = 10$ period plotting for $l_{\text{full}} \simeq 500$ length curves and by $k = 50$ period plotting for $l_{\text{full}} \simeq 2500$ length curves. The case (b) becomes only $k = 10$ plotting for $l_{\text{full}} \simeq 4.45 \times 10^5$. The case (c) becomes $k = 10$ plotting for $l_{\text{full}} \simeq 676$ and $k = 50$ plotting for $l_{\text{full}} \simeq 3381$.

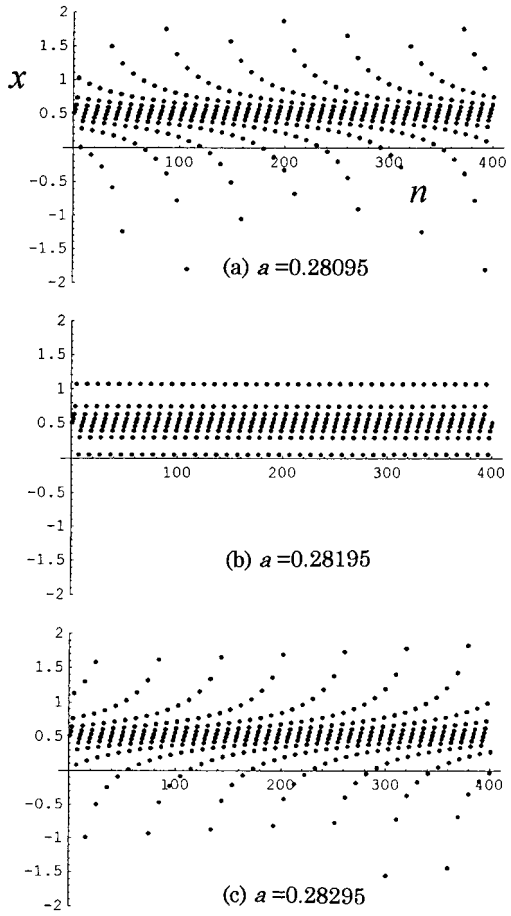

Fig. 5. Alternate x_n distributions in the continued fractions ($b = 1.01$). Many tangent curves can be traced for up and down directions in each graph. In (a) and (c), two kinds of plotting ($k = 10$ and 50 periods) can be directly traced. In these cases, small values λ_k appear as (a) $\lambda_{10} = -0.389$ and (c) $\lambda_{10} = 0.278$, respectively, at $k = 10$. In (b), the small value $\lambda_{10} = 0.00043$ appears as the case closing to the cycle condition of $a = 0.281949\cdots$.

2.4.2. Attractor and repellor

As for simple continued fractions, the attractor points are produced in large x area under the condition of Eq. (15):

$$|q'_k(x)| < 1, \quad |1 - \lambda_k x| > 1. \tag{30}$$

However, such a condition is meaningless for the following reasons. After x_n steps cross the number b, the values at the next step are large ($|x_{n+1}| \gg 1$). Equation (30) seems to be satisfied in these steps, although, the values at step $n+2$ are small ($x_{n+2} \approx 0$), and the values for subsequent steps are all similar values ($x_{n+3} \approx a/b$). In any case, the continued fractions return to ordinary sequences.

2.4.3. The Cauchy distribution

The probability density of x in the continued fraction is calculated from Eq. (29). The number x_{n+k} appears once every k times with the small distance Δ_k. Hence, from Eqs. (14), (27) and (29), the density at an arbitrary point x_{n+k} is proportional

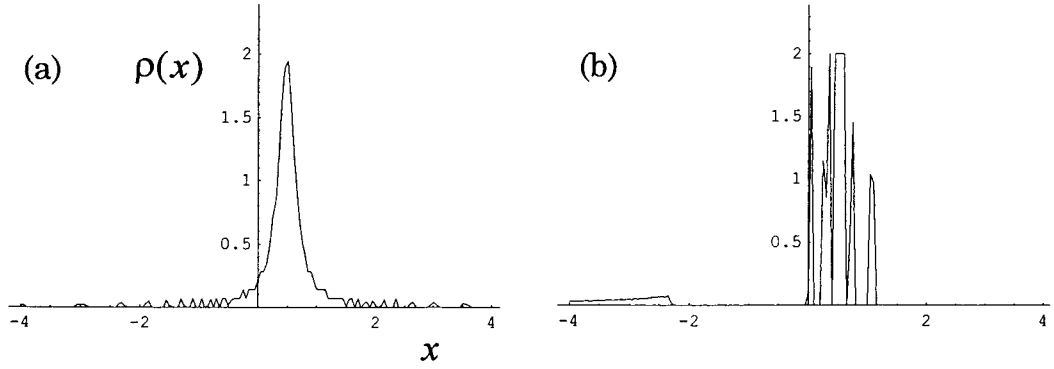

Fig. 6. Cauchy distributions of the examples in Fig. 5. (a) Clear distribution with $\xi = 0.505$, $\eta = 0.161$ and $\lambda = -0.389$. (b) Slow configuration with $\xi = 0.505$, $\eta = 0.164$ and $\lambda_k = 0.00043$.

to $1/\Delta_k$:

$$\rho_k(x) \propto \sum_{i=1}^{k} \frac{1}{k|\Delta_k|} \approx \frac{1}{\Delta_k} = \left|\frac{1}{\lambda_k}\right| \frac{1}{(x-\xi)^2 + \eta^2}. \tag{31}$$

We can consider a series with arbitrary k period, where the sign of the small distance Δ_k becomes arbitrary. For large x, x in the denominator of Eq. (14) vanishes, as the result of the averaging manipulations and the sufficiently small λ_k. Considering the normalization condition, the density function is obtained finally as the Cauchy distribution in Fig. 6 for a infinite iterations:

$$\rho(x) = \frac{1}{\pi} \frac{\eta}{(x-\xi)^2 + \eta^2}. \tag{32}$$

2.4.4. Self-energy and the Green's function

In the infinite case, we can analyze the probability densities using the Green's functions. The electronic state densities are calculated from the secular equations by means of the LCAO method. In this method, Eq. (3) represents a linear chain and Eq. (4) represents a Bethe lattice. The formulas in the LCAO theory all belong to the group of the linear (symmetric) algebraic equations.[7] All of the secular equations can be approximately transformed into a linear chain formula in infinite systems.[8) - 10)]

The distribution behavior of the continued fractions is determined by the cyclic terms, as explained in the above section. Under these cycle conditions, we can discuss the state density calculations. Equation (32) and the basic equations (12)–(14) can be analyzed using a Green's function:

$$G_k(x) = \frac{1}{\Delta_k} = \frac{1}{x - q_k(x)} \Rightarrow \frac{1}{x - \sigma(x)}. \tag{33}$$

This Green's function gives information of the cyclic terms induced from Λ_k in Eq. (21) for the parameters a and b, where the value x is arbitrary.

If the simple continued fraction is in a distribution state, $q_k(x)$ becomes the

complex number self-energy σ in the Green's function:

$$\sigma = \frac{a}{b-\sigma} = \xi \pm i\eta. \tag{34}$$

The probability density is calculated from this Green's function using the positive imaginary σ:

$$\rho(x) = \frac{1}{\pi}\mathrm{Im}G(x) = \frac{1}{\pi}\mathrm{Im}\frac{1}{x-\sigma}. \tag{35}$$

If σ is a real constant, this function becomes the δ-function, as is well known. This δ-function also represents the cyclic terms accompanied by the bifurcations as the chaotic behavior in the logistic map. In §3, we attempt to approximately draw the densities of the logistic map using such a calculation method.

2.4.5. Tangent function

The various slow curves of dots in Fig. 4 represent tangent functions. Let l be the iteration length (real number) for the iteration times k,

$$l(\text{length}) = k(\text{times}).$$

Then the change of x for l can be obtained from Eqs. (14) and (29):

$$\frac{dx}{dl} \approx \frac{x_{n+k} - x_n}{k} \approx \frac{\lambda_k(x^2 - bx + a)}{k}. \tag{36}$$

From this equation, the length is determined as

$$\int_{l_{-\infty}}^{l} dl = l - l_{-\infty} = \frac{k}{\eta\lambda_k}\int_{-\infty}^{x} \frac{\eta}{(x-\xi)^2 + \eta^2}dx.$$

The length l for the variable x becomes the Cauchy distribution function (Heaviside step function):

$$l - l_{-\infty} = \frac{\pi k}{\eta\lambda_k}F(x) = \frac{k}{\eta\lambda_k}\Big\{\tan^{-1}\frac{x-\xi}{\eta} + \frac{\pi}{2}\Big\}. \tag{37}$$

From this result, the change of x in terms of l is represented by the tangent function:

$$x = \xi + \eta\tan\left[\frac{\eta\lambda_k(l - l_{-\infty})}{k} - \frac{\pi}{2}\right]. \tag{37}'$$

The full length of one tangent function becomes

$$\begin{aligned} &l_{\text{full}} = l_\infty - l_{-\infty} = \frac{\pi k}{\eta\lambda_k}, \\ &-\infty < \tan\theta < \infty, \quad -\frac{\pi}{2} < \theta < \frac{\pi}{2}. \end{aligned} \tag{38}$$

In Fig. 5(a), for the values $a = 0.28095$, $b = 1.01$, $\eta = 0.161$, $k = 10$ and $\lambda_k = -0.389$, the full length number becomes $l_{\text{full}} = 501.6$.

§3. Logistic map

3.1. *Basic equation*

The well-known logistic map [3) - 5)] is discussed in this section for characterizing continued fractions. The logistic map equation

$$X_{n+1} = RX_n(1 - X_n) \tag{39}$$

can be rewritten as one of the continued fraction groups ($a = 0,\ b = 1,\ c = 0,\ d = -1,\ e = 1$ in Eq. (2)). Although this equation differs from the simple continued fraction because of the asymmetrical term $d < 0$, the chaotic behavior can be analyzed using a method similar to the Cauchy distributions. In this work, the logistic map equation is distinguished into the cycle equations

$$X_{n+k} = Q_k(X_n) = X_n, \tag{40}$$

which correspond to the cycle equations of Eq. (21) in the continued fractions. All of these algebraic equations were directly solved numerically. The maximum of the cycle number ($k \approx 6$) is determined by the numerical precision (more than 16 digits) of the computing processes.

3.2. *Convergence*

For Eq. (40) with $k = 1$, the convergent condition in the logistic map becomes

$$\left|\frac{\delta}{\varepsilon}\right| = |R(1 - 2X)| \leq 1, \tag{41}$$

as discussed in §2 using Eqs. (15) and (19). With this condition, setting $X_0 = X$, the solutions of the quadratic equation Eq. (39) are obtained as

$$\begin{aligned} X &= 0 \qquad\qquad \text{for } \ 0 < R \leqq 1, \\ X &= \left(1 - \frac{1}{R}\right) \ \text{ for } \ 1 < R \leqq 3, \end{aligned} \tag{42}$$

reproducing known results.[3)] These results are similar to those for the simple continued fractions.

3.3. *Cycle*

Like Eq. (21) discussed in §2, the cycle equation in the logistic map becomes Eq. (40), where the conditions

$$\begin{aligned} &3 < R \leqq 4, \\ &X_{n+1} \neq X_n \end{aligned} \tag{43}$$

are satisfied. Such conditions have been studied, and various results are known. [3) - 5)] In these results, the stable sequence (*attractor*) condition

$$\left|\frac{\delta}{\varepsilon}\right| = |Q_k'(X)| < 1 \tag{44}$$

is used in the calculations.

The quadratic equations of the cyclic terms become the high-degree algebraic equations (43) along with the iteration times. The real-number solutions ξ_i in these equations are transformed into the square root of the density function as the broadened δ-function:

$$\left|\frac{1}{X-\xi_{k,i}}\right| = \frac{1}{\sqrt{(X-\xi_{k,i})^2+\varepsilon^2+\mu}}. \tag{45}$$

We use $\varepsilon = 10^{-2}$ in this work. In such calculations, repellors and attractors are considered by introducing the factor μ, using Eq. (44). This function μ destroys the repellor point delta-function and does not effect the other point mapping functions:

$$\mu = \begin{cases} 0 : |Q'| < 1 & \cdots \text{attractor}, \\ 1 : |Q'| > 1 & \cdots \text{repellor}. \end{cases} \tag{46}$$

By means of this function, we can control the densities of the repellor points to be non-effective. Equation (44) is numerically solvable until $k \sim 6$ with 16 digit precision.

3.4. *Distribution*

The behavior of the distributions appears as breaking of the cycles. We obtain real and complex number solutions for Eq. (40). The real solutions represent the cyclic terms (accompanied by the bifurcation) which are quite different from those in the simple continued fraction. The complex solutions directly indicate the distribution phenomena in the iterated values, like the Cauchy distribution in §2.

We have the stable (attractor) distribution conditions as the well-known results [3) - 5)] in the logistic map:

$$\begin{aligned} &3 < R \leqq 4, \\ &X_{n+k} - X_n = \Delta_k \neq 0, \\ &|Q'_k(X)| \leq 1. \end{aligned} \tag{47}$$

Equation (39) is a real value mapping on the real axis from 0 to 1. At the first step, the values X_1 are mapped from the values X_0 from 0 to 1:

$$RX_0(1-X_0) \to X_1.$$

Here the real values X_0 and X_1 satisfy the equation

$$X_0^2 - X_0 + \frac{X_1}{R} = 0, \tag{48}$$

and the real X_0 must be equated as a real value in Eq. (48):

$$1 - \frac{4X_1}{R} > 0 \to X_1 < \frac{R}{4}. \tag{49}$$

This is the first restriction. From the next step equation

$$X_1^2 - X_1 + \frac{X_2}{R} = 0, \tag{50}$$

the following relation is obtained:

$$\frac{R}{4} > X_1 = \frac{1}{2}\left(1 \pm \sqrt{1 - \frac{4X_2}{R}}\right). \tag{51}$$

In this relation, the values X_2 have the second restriction

$$\begin{aligned} &\frac{R}{4} - \frac{1}{2} > \sqrt{1 - \frac{4X_2}{R}} > 0, \\ &\frac{R}{4}\left[1 - \left(\frac{R}{4} - \frac{1}{2}\right)^2\right] < X_2 \end{aligned} \tag{52}$$

for the (+) root and

$$\begin{aligned} &0 < \frac{1}{2} - \frac{R}{4} < \sqrt{1 - \frac{4X_2}{R}}, \\ &\frac{R}{4}\left[1 - \left(\frac{1}{2} - \frac{R}{4}\right)^2\right] > X_2 \end{aligned} \tag{53}$$

for the (−) root. Such followed restrictions for $X_{n+1},\ X_{n+2}\ \cdots$ also exist in the continued sequence:

$$\begin{aligned} &F_1 = \frac{R}{4}, \quad F_{n+1} = \frac{R}{4}[1 - (2F_n - 1)^2], \\ &F_n > X_n = \frac{1}{2}\left(1 + \sqrt{1 - \frac{4X_{n+1}}{R}}\right), \\ &F_n < X_n = \frac{1}{2}\left(1 - \sqrt{1 - \frac{4X_{n+1}}{R}}\right). \end{aligned} \tag{54}$$

Here the inequalities are changed by the previous step inequality and $\pm$ sign (larger or smaller than 1/2). These restricted values F_n imply important rules in the logistic map.

If the value Δ_k in Eq. (44) is small but nonzero, the analysis in the continued fractions can be adapted similarly for this case, where the complex-numbers σ are determined by the equation

$$\sigma_{k,m} = Q_k(\sigma_{k,m}) = \xi_m + i\eta_m. \tag{55}$$

The cycle equations of the logistic map can be equated using these solutions including the real numbers

$$X - Q_k(X) = \prod_{i=1}^{2^k}(X - \sigma_{k,i}), \tag{56}$$

which are represented in a multiplied form of the quadratic functions. In this work, as a first approximation, the density functions are equated like Eqs. (28), (31) and

(32) in the continued fractions:

$$\rho_k(X) \propto \frac{1}{|\Delta_k|} = \frac{1}{|X - Q_k(X)|} = \frac{1}{\left|\prod_{i=1}(X - \sigma_{k,j})\right|}. \tag{57}$$

This equation implies that the logistic map is characterized by the quadratic functions including the Cauchy distributions. There is also a related argument.[4)]

In practical calculations, we must consider the basic foundations as follows. The distribution range is from 0 to 1, and the values Δ_k are produced around the specific attractors at X_a. The probability densities ρ_k are inherited in the next mapping from k to $k+1$. If the attractive areas around X_a are continuously mapped into the next attractive areas, the high-density parts are continued as areas. If the repetitious mapping includes the repellor area, the high-density mapping is broken. These relations are self-consistently formed in the continued mapping.

With the above considerations, we attempt to approximate the density function of the logistic map using the k-th X areas from F_k^a to F_k^b determined by Eq. (54):

$$\rho_k(X) \approx h_k \prod_{i=1}^{2^k} \frac{1}{[(X - \xi_{k,i})^2 + \eta_{k,i}^2 + \mu_{k,i}]^{0.5}} \quad \text{for} \quad F_k^a < X < F_k^b. \tag{58}$$

Here, the real value solutions are treated as in Eq. (45). The form of Eq. (58) is almost the same as Eq. (57), except for the normalization constant h_k and the repellor function $\mu_{k,i}$.

The continued attractor sequence is restricted in the iteration regions as in Eq. (54). Almost one or two of these attractor points $\xi_{k,i}$ exist in every k cycles and are concentrated in the edge regions. Thus, the high-density parts continue in the restricted edge regions. The actual repellor point distributions are broadened in continued iterations. Although some of them (e.g. $R = 3.8$, $x = 0.33$) are not completely destroyed in our calculation. Under these relations, the high-density parts must be destroyed in the k-th cycle roughly with the ratio

$$\text{Destroyed ratio} \propto \frac{1}{k-2}. \tag{59}$$

The total distribution density is obtained by superposing each cycle as an approximation:

$$\rho(X) = \sum_k \frac{1}{k-2}\rho_k(X). \tag{60}$$

The results appear in Fig. 7. This approximation is very rough, and the re-

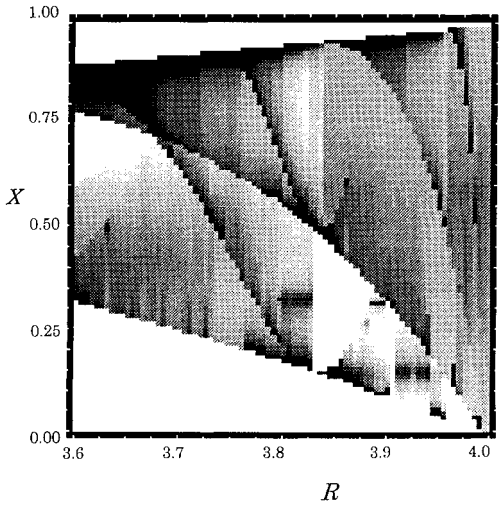

Fig. 7. Density representation of the logistic map.

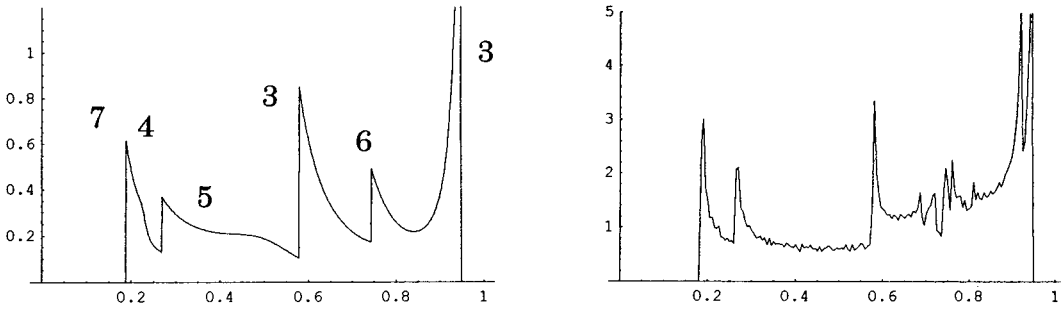

(a) Calculation **(b) Iteration**

Fig. 8. Comparison of the distribution densities for $R = 3.79$. (a) The cycle equations are considered for $k = 3$–7 in Eq. (58). The peaks are numbered by k. (b) Large peaks appear at the band edges in the numerical iteration results.

sults are not self-consistent, where the cycle equations are taken into account from $k = 3$ to 6.

The calculated distribution densities at $R = 3.79$ are presented in Fig. 8 and compared with the numerical results of the iterations to show the degree of precision. In the numerical iteration results, the large peaks indicate the band edge distributions of each cycle, which is observed from $k = 3$ to about 10. In Fig. 8 (a) the density calculations are performed for $k = 3$ to 7. Here, the lack of peaks of higher order cycles ($k = 8$–10) is noteworthy around $x = 0.7$–0.8.

§4. Conclusion

The various properties of chaotic and chaos-like behavior in continued fractions have been clarified. In the chaos-like behavior, the double Markov sequences dominate the map in the Cauchy distribution areas where the real numbers are distributed along with many tangent functions. The distribution density of the logistic map has been analyzed, where the Green's function theory was manipulated like the calculations of electronic state densities in solids. From these results, it has been pointed out that the distribution phenomena are commonly based on the Cauchy distributions in these continued fraction maps.

Acknowledgements

The authors thank Professor H. Daido (Kyushu I. T.) for conceptual advice on this paper in its early days. They are grateful to the Tokyo Denki University Computer Center for providing unlimited use of computing facilities.

References

1) S. Obata, S. Ohkuro and T. Maeda, Prog. Theor. Phys. **101** (1999), No. 5.
2) M. Schroeder, *Fractals, Chaos, Power laws* (W. H. Freeman & Company, New York, 1991).

3) D. Gulick, *Encounters with Chaos* (McGraw-Hill, Inc., 1992).
4) D. J. Scalapino, J. E. Hirsch and B. A. Huberman, in *Melting Localization and Chaos*, ed. R. K. Kalia and P. Vashishta (North-Holland/Elsevier Science, Inc., 1982), p. 243.
5) M. Barnsley, *Fractals Everywhere* (Academic Press, Inc., 1988).
6) T. Matsumoto and Y. Aizawa, Prog. Theor. Phys. **97** (1997), 739.
7) R. Haydock, V. Heine and M. J. Kelly, J. of Phys. **C5** (1972), 2845.
8) S. Obata, J. Phys. Soc. Jpn. **58** (1989), 4257.
9) S. Obata, J. Phys. Soc. Jpn. **60** (1991), 65.
10) S. Obata and S. Shinohara, J. of Phys. **C13** (1980), 1257.